

Measurement of Ambient, Interstitial, and Residual Aerosol Particles on a Mountaintop Site in Central Sweden using an Aerosol Mass Spectrometer and a CVI

Frank Drewnick · Johannes Schneider · Silke S. Hings ·
Nele Hock · Kevin Noone · Admir Targino ·
Silke Weimer · Stephan Borrmann

Received: 6 September 2005 / Accepted: 6 July 2006
© Springer Science + Business Media B.V. 2006

Abstract The Aerodyne aerosol mass spectrometer (Q-AMS) was coupled with a counterflow virtual impactor (CVI) for the first time to measure cloud droplet residuals of warm tropospheric clouds on Mt. Åreskutan in central Sweden in July 2003. Operating the CVI in different operational modes generated mass concentration and species-resolved mass distribution data for non-refractory species of the ambient, interstitial, and residual aerosol. The ambient aerosol measurements revealed that the aerosol at the site was mainly influenced by long-range transport and regional photochemical generation of nitrate and organic aerosol components. Four different major air masses were identified for the time interval of the experiment. While two air masses that approached the site from northeastern Europe via Finland showed very similar aerosol composition, the other two air masses from polar regions and the British Islands had a significantly different composition. During cloud events the larger aerosol particles were found to be activated into cloud droplets. On a mass

F. Drewnick (✉) · J. Schneider · S. S. Hings · N. Hock · S. Borrmann
Particle Chemistry Department, Max-Planck Institute for Chemistry,
J. J. Becherweg 27, D-55128 Mainz, Germany
e-mail: drewnick@mpch-mainz.mpg.de

F. Drewnick · S. S. Hings · N. Hock · S. Weimer · S. Borrmann
Institute for Atmospheric Physics, University of Mainz, J. J. Becherweg 21, D-55128 Mainz, Germany

K. Noone · A. Targino
Department of Applied Environmental Science, Stockholm University, SE-10691 Stockholm, Sweden

S. Weimer
EMPA, CH-8600 Dübendorf, Switzerland

S. Weimer
Paul Scherrer Institute, CH-5232 Villigen, Switzerland

basis the activation cut-off diameter was approximately 150 nm for nitrate and organics dominated particles and 200 nm for sulfate dominated particles. Generally nitrate and organics were found to be activated into cloud droplets with higher efficiency than sulfate. While a significant fraction of the nitrate in ambient particles was organic nitrates or nitrogen-containing organic species, the nitrate found in the cloud droplet residuals was mainly ammonium nitrate. After passage of clouds the ambient aerosol size distribution had shifted to smaller particle sizes due to the predominantly activation of larger aerosol particles without a significant change in the relative composition of the ambient aerosol.

Key words AMS · aerosol activation · CVI · scavenging

1 Introduction

Aerosol–cloud interactions are the basis for a number of fundamental processes in the atmosphere. Although the influence of aerosol particles on climate forcing is widely recognized, the magnitude of this contribution is still unknown and is one of the largest uncertainties in the prediction of anthropogenic influences on climate change (Houghton et al., 2001). Currently it is assumed that the combination of aerosol direct and indirect effects contributes to climate forcing potentially in the same magnitude but in opposite direction as greenhouse gas forcing. Aerosol climate forcing splits into direct and indirect effects with the major uncertainty lying in the latter category. Direct effects are scattering and absorption of incoming and outgoing radiation by aerosol particles while indirect effects are interaction of radiation with clouds, which are largely influenced by aerosol properties. Cloud droplets form on pre-existing particles, known as cloud condensation nuclei (CCN). As a consequence, anthropogenic activities that increase aerosol concentrations may lead to more reflective clouds by increasing the amount of CCN and therefore of cloud droplets (Twomey, 1977). In addition increased concentrations of CCN and as a consequence more but smaller cloud droplets could delay the formation of precipitation, which would increase the lifetime of the clouds (Albrecht, 1989).

In order to reduce the uncertainty of the climate impact of aerosol particles, the details of the hydrological cycle need to be investigated in detail. All individual cloud droplets start their life as aerosol particles. Thus, at the most fundamental level, understanding the processes that determine cloud properties—both physical and chemical—requires understanding which particles, out of all those that are present in the atmosphere, actually form cloud droplets under various different conditions.

A major challenge in acquiring this understanding is the fact that cloud droplets are the result of water vapor condensing on individual aerosol particles. Understanding what controls cloud properties like albedo or precipitation development requires, as a first step, knowing what causes certain particles to activate and form cloud droplets, while other particles in the same cloud do not. Therefore, aerosol–cloud interactions need to be investigated on a very fundamental level.

Experimental studies to acquire information about aerosol–cloud interaction have often used a Counterflow Virtual Impactor (CVI) to separate cloud droplets from the interstitial aerosol (Ogren et al., 1985; Noone et al., 1988; Gieray et al., 1989; Hallberg et al., 1994; Noone et al., 2000). In recent years, on-line aerosol mass spectrometry has advanced to become a powerful tool in the physical and chemical analysis of individual aerosol particles and small particle ensembles. An example of these instruments is the Aerodyne aerosol mass spectrometer (Q-AMS) that is capable of quantitatively measuring the non-refractory

aerosol composition of sub-micrometer particles and species-resolved mass distributions of these components (Jayne et al., 2000; Jimenez et al., 2003a).

An experiment to determine microphysical and chemical interactions between aerosol particles and cloud droplets was carried out during July 2003 at Mt. Åreskutan in central Sweden (SOACED, sources and origin of atmospheric cloud droplets). Here, for the first time an Aerodyne aerosol mass spectrometer (Q-AMS) was coupled to a Counterflow Virtual Impactor in order to measure cloud droplet residuals. The aim of this project was to compare the chemical and physical properties of ambient, interstitial, and residual aerosol particles to better understand the processes that determine the uptake of particles into cloud droplets. Here we report on the results of the aerosol mass spectrometer measurements from this campaign.

2 Instrumentation and Measurements

The measurements presented here were performed in a cabin operated by the Institute of Applied Environmental Research of Stockholm University on Mt. Åreskutan (63.43°N, 13.08°E) at an elevation of 1,270 m a.s.l. Mt. Åreskutan is located in Jämtland in central Sweden about 100 km west of Östersund and 600 km northwest of Stockholm. The mountain is surrounded by other mountains of similar or slightly less elevation with extended forests below the timberline (1,000 m a.s.l.) and small lakes in the valleys. The area has almost no industry or other significant anthropogenic emitters of particulate matter. The closest village is Åre with about 1,000 inhabitants, in the valley approximately 850 m below the site. This village is crossed by the E14, the only larger road in that region that connects Östersund and Trondheim (Norway). The only near-site source of anthropogenic emissions is the kitchen of a small restaurant, which is located in the top station of an electrical cable car, about 100 m east and 10 m above the sampling station. However, the emissions from this source should typically pass over the sampling probes of the site and could only reach the station at wind directions between 70° and 110°, which were rarely observed during the campaign.

The measurement site on Mt. Åreskutan is a well-characterized location for investigation of clean continental clouds (Ogren et al., 1989; Noone et al., 1991), which can be expected to be within clouds on a frequent basis during the summer months. In addition the aerosol and cloud measurements at this location were supported by local meteorological measurements at the summit of Mt. Åreskutan (WMO measurement site #02215), approximately 1 km northeast and 150 m above the measurement site.

The measurement cabin was a wooden construction with a size of 3.6×5.1 m. The cabin was equipped with two main aerosol inlets: an interstitial inlet and the CVI inlet. The interstitial inlet consisted of a radial impactor that was designed to remove particles larger than 5 μm in diameter. During cloud events the cloud droplets were removed by the impactor and only the interstitial aerosol was measured. During the remaining time the ambient aerosol (smaller than 5 μm) was measured. The second sampling inlet was the Counterflow Virtual Impactor (CVI, Noone et al., 1988). The CVI wind tunnel and probe were located at a height of approximately 4 m above ground level 30 cm below a 1.5 m² plate. Here the collected air was accelerated to a velocity of 100 m s⁻¹ before it was directed onto the CVI probe. The probe consists of two concentric tubes, joined at the probe tip. The outer probe is solid, and the last 10 cm of the inner tube are porous. The centerline of the probe is oriented parallel to the trajectories of the droplets in the wind tunnel. Filtered, dried, and heated air is pumped through the annular space between the two tubes

and passes through the porous inner tube. Part of this flow leaves the inner tube in the opposite direction of the arriving aerosol particles and forms the counterflow that separates large particles from those below a cut-off diameter. The remaining part of the flow makes up the sample flow in which the sampled cloud droplets evaporate and the remaining residual particles were transported to the connected instruments. During this experiment the flow rates of the CVI were selected such that particles or cloud droplets with diameters of 5 μm or more were collected and smaller particles were removed by the counterflow. By turning off the wind tunnel and the counterflow the CVI can be used as ambient aerosol inlet. During cloud events in this sampling mode cloud droplets were removed from the sampled aerosol by impaction onto the walls of the bends in the sampling line, so that effectively the interstitial aerosol was collected.

The CVI sample flow was split into sub-flows to serve a number of instruments that measured physical and chemical aerosol parameters, including particle number concentration (CPC), particle size distribution (SMPS), optical particle properties (nephelometer and soot photometers) and size-resolved chemical composition of the particles (Q-AMS). Here we focus on real-time measurements of species- and size-resolved aerosol mass concentrations performed with the Aerodyne aerosol mass spectrometer (Q-AMS) and of particle number concentration measurements using a TSI Model 3025 condensation particle counter.

The aerosol mass spectrometer (Q-AMS) used during SOACED collects and focuses particles in the size range of $d_p = 40$ to 1,000 nm into a narrow beam using an aerodynamic lens assembly. After passing through a particle time-of-flight chamber and an aperture the particles impact onto the vaporizer, a porous tungsten surface, heated to approximately 530 °C. The non-refractory particle components flash-evaporate and the evolving vapor is ionized by electron impact ($E = 70$ eV). The ions are extracted into a quadrupole mass spectrometer and detected after mass analysis using an electron multiplier. A comprehensive description of the Q-AMS is given in (Jayne et al., 2000 and Jimenez et al., 2003a), a description of the vaporizer and the ionizer is given in (Drewnick et al., 2005).

The Q-AMS measures in two modes of operation: In the *mass spectrum (MS) mode* the particle beam completely passes to the vaporizer for 5 s and then is completely blocked for another 5 s. During each of these time intervals the whole mass spectrum (1–300 amu) is scanned 15 times by the quadrupole mass spectrometer, measuring the average aerosol and background mass spectra. The aerosol mass spectrum is then determined by calculating the difference of these spectra. From this difference spectrum the mass concentrations of non-refractory aerosol components sulfate, nitrate, ammonium and total organics are calculated using the inversion algorithm described by Allan et al. (2004).

The second mode of operation is the *time-of-flight (TOF) mode*, where particle time-of-flight measurements are used to determine particle size. In this mode the particle beam is chopped with a frequency of ~ 100 Hz using a chopper wheel at the beginning of the particle time-of-flight chamber. The chopper has two radial slits comprising 2% of the wheel area, defining a common starting time for all particles at each chopper cycle. The quadrupole mass spectrometer is set to measure at an individual m/z and synchronized with the chopper rotation so that the detector signal is recorded as a function of particle flight time. Using a particle time-of-flight (P-ToF) calibration the particle flight time is converted into a vacuum aerodynamic diameter, resulting in a mass size distribution for the measured m/z of the species that are related to this m/z . The vacuum aerodynamic diameter d_{va} is defined as the aerodynamic equivalent diameter measured in the molecular flow regime. Due to the proportionality of the Cunningham slip correction C_c to the inverse of the particle diameter in this flow regime, d_{va} is directly proportional to the ratio of particle

density to particle shape factor – while the classical aerodynamic diameter is proportional to the square root of this ratio. A detailed description and derivation of the vacuum aerodynamic diameter can be found in (Jimenez et al., 2003b, and DeCarlo et al., 2004).

During the measurements presented here the Q-AMS was operated in an alternate mode, switching between MS- and TOF-mode every 20 s. Averaged mass spectra and size distributions were saved every 10 min. The m/z (and related species) selected in TOF-mode were 16/17 (ammonium), 18 (water), 28 (air, used for monitoring the multiplier performance), 30/46 (nitrate), 48/64 (sulfate), and 43/44/55/57/69/71 (organics). The Q-AMS measurements started in the afternoon of July 1st and were terminated in the morning of July 29. During the week from the evening of July 9 until the morning of July 16 no measurements have been made with the Q-AMS due to a failure of the ion source power supply. In addition during several nights the Q-AMS measurements have been interrupted to avoid overheating of the pump system, because the measurement cabin was not equipped with any active air-cooling. During daytime cooling was provided by opening the windows or the cabin door. These interruptions together with data loss during times where the CVI was operated in undefined states or switched between operation modes within a 10-min Q-AMS cycle resulted in a useful data coverage of 46% of the total time of the campaign.

For quality assurance of the Q-AMS measurements a series of calibrations have been performed before and during the campaign. The ionization and transmission efficiency of the Q-AMS ionizer was calibrated in the laboratory before transport to the measurement site; at the site the gain of the electron multiplier was calibrated before the beginning of the measurements and several times during the campaign. Because the inlet flow characteristics of the Q-AMS are changed under the reduced pressure conditions on Mt. Åreskutan compared to the lab conditions an inlet flow calibration that relates the pressure measured in the inlet system and the inlet flow rate was performed at the measurement site before the measurements started. Also the particle time-of-flight calibration that is used to calculate the particle vacuum aerodynamic diameter from the measured flight time depends on ambient pressure. Since this calibration could not be performed at the site the P-TOF calibration parameters have been calculated from pressure-dependent particle time-of-flight measurements, performed in the laboratory (Schneider et al., 2006a).

The main uncertainties in the quantification of the Q-AMS mass concentration measurements are the ionization and transmission efficiency calibration and the correction for particle losses in the instrument due to bounce from the vaporizer (collection efficiency, CE = 0.5), resulting in an overall uncertainty of the absolute Q-AMS mass concentrations in the order of 25%. However, since both factors, ionization efficiency and collection efficiency affect all measurements in the same manner, the reproducibility and thus the relative mass concentrations determined with the Q-AMS have a much lower uncertainty in the order of 5% with slightly larger uncertainties in the ammonium measurement due to significant contribution of water- and air-related signal to the ammonium fragment m/z . In this study mainly relative mass concentrations are used to extract conclusions and thus the latter uncertainty is relevant to these measurements. Minimum detection limits for the individual species are mainly determined by counting statistics and electronic noise. In earlier campaigns the 10-min average detection limits have been estimated to be in the order of 0.1–0.25 $\mu\text{g m}^{-3}$ for the inorganic species and around 1 $\mu\text{g m}^{-3}$ for the organics, which have a significantly higher noise level due to the large number of m/z contributing to this species (Drewnick et al., 2004). The uncertainty of the particle size measurement is mainly determined by the finite opening time of the chopper wheel (2% duty cycle), the time resolution of the data acquisition (50 μs , $\sim 1\%$ of particle time-of-flight) and the uncertainties of the P-TOF calibration ($\sim 5\%$), resulting in an overall uncertainty of the measured

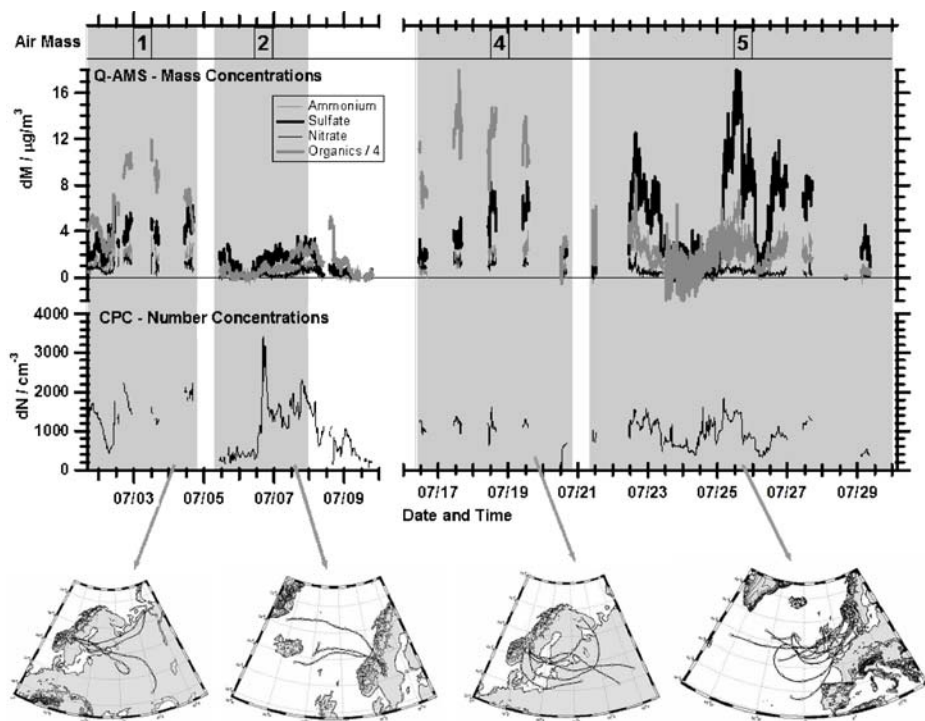


Figure 1 Time series of nitrate, sulfate, ammonium, and organics mass concentrations measured with the Q-AMS (*upper traces*) and particle number concentrations measured with a CPC (*lower trace*). The time axis is cut to avoid large empty space due to Q-AMS ion source power supply failure in the middle of the campaign. During the Q-AMS measurements four distinguishable air masses were identified (#1, 2, 4, and 5). A set of back trajectories with one trace for each day is shown for the four air masses at the bottom of the panel.

particle sizes in the order of slightly more than 5%. Uncertainties in the particle flight time measurement due to the finite evaporation time of the particles are accounted for by the P-TOF calibration for typical aerosol components. Due to the low chopper duty cycle (2%) and the distribution of the measured ions into approximately 80 size bins the detection limits for the size distributions are somewhat larger than those for the mass concentrations. Taking into account the different timing scheme in the P-TOF measurements compared to the MS measurements the size distribution LODs are estimated to be in the order of 2–5 $\mu\text{g}/\text{m}^3$ for the individual species for 10-min averaged size distributions.

3 Results and Discussion

3.1 The ambient aerosol at Mt. Åreskutan

As an overview time series of the sulfate, nitrate, ammonium, and total organics mass concentrations measured with the Q-AMS during the whole campaign are shown in Figure 1 together with total aerosol number concentrations measured with the CPC. The individual species concentrations showed no distinct diurnal variation, suggesting that no

Table I Description of the five air masses that arrived at the measurement site during the campaign

Air mass #	Arrival time	Description of path
1	07/01–07/04	NE Europe – S-Finland
2	07/05–07/07	Polar Sea – across Norway
3	07/09–07/15	North Atlantic – across Norway
4	07/16–07/20	NE Europe – S-Finland
5	07/21–07/29	British Islands

local particle production or local wind patterns existed that generated or advected increased particle concentrations at any time of the day on a regular basis.

The aerosol mass concentrations displayed in Figure 1 show variations on time scales of several days, indicating that the aerosol is largely influenced by regional or long-range transport rather than local effects. Back trajectories calculated for every day for a 12:00 UTC arrival time at the measurement site using the McGrath (1988) model of the European Center of Medium-range Weather Forecasts revealed that the air at the site could be roughly divided into five air masses of different origin. The five air masses and their arrival time intervals at the measurement site are described in Table I. Since significant data of Q-AMS measurements only exist during air mass #1, 2, 4, and 5 we will only use these air masses for further discussion. For each of these air masses a set of back trajectories (one for each day) is included in Figure 1.

The average composition of the non-refractory aerosol measured with the Q-AMS was determined for each of the air masses individually. The mass concentrations for each of the species are given in Table II. The largest mass concentrations are found in air mass #1 and 4, the two air masses that approached the measurement site via northeast Europe and Southern Finland. The lowest mass concentrations were found in air mass #2, which was composed of polar air that traveled across Norway before it arrived at the site. The relative composition of each of the air masses is shown in pie charts in Figure 2. Again the two air masses that had similar origin and had the largest mass concentrations – air mass #1 and 4 – are very different from the other air masses and very similar to each other. These two air masses both have an extremely high organic mass fraction of 80% or larger, while for the air masses #2 and 5 the organic mass content is 52% and 49%, respectively. Accordingly the sulfate and ammonium content in air masses #1 and 4 are low compared to those in the other two air masses. The nitrate content is in the order of 2%–3% in all air masses.

The average compositions of the aerosol in the four air masses as shown in Table II and Figure 2 show that all three air masses that passed over continental Europe or the British

Table II Mass concentrations for each of the non-refractory species measured with the Q-AMS during the time intervals of the four air masses

Air mass	#1: 7/01–7/04 S-Finland, NE-Europe ($\mu\text{g m}^{-3}$)	#2: 7/05–7/07 Polar Air, Norway ($\mu\text{g m}^{-3}$)	#4: 7/16–7/20 S-Finland, NE-Europe ($\mu\text{g m}^{-3}$)	#5: 7/21–7/29 British Islands ($\mu\text{g m}^{-3}$)
Nitrate	0.9	0.1	1.0	0.4
Sulfate	3.2	1.2	3.8	5.4
Ammonium	1.6	0.5	1.5	1.9
Chloride	0.04	0.02	0.04	0.01
Organics	24	2.0	39	7.3
Total	29	3.9	46	15

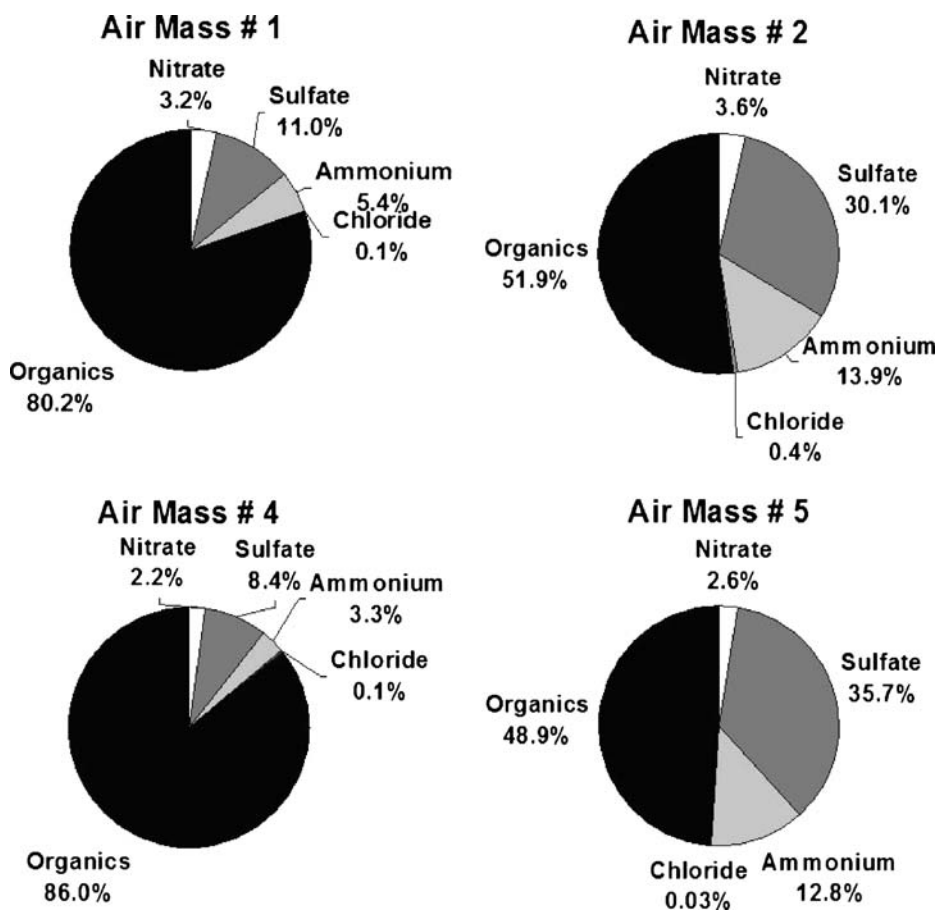
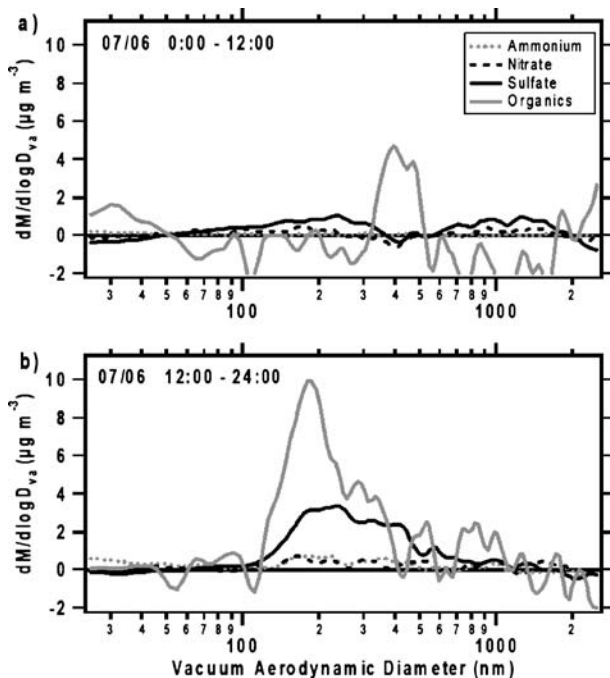


Figure 2 Composition of the ambient aerosol during each of the four air masses. Air mass #1 and 4 both approached the measurement site coming from Eastern Europe via Finland; air mass #2 consisted of polar air that only crossed through Norway; air mass #5 came over the British Islands.

Islands had significant sulfate concentrations; however, in the two air masses that passed over Southern Finland extremely large organics mass concentrations were found, resulting in a domination of the aerosol by organic compounds. This might be due to generation of organic particles or condensational growth of particles as a result of photooxidation of terpenes and other vapors known to be emitted in large amounts by the Finnish forests (Kulmala et al., 2004). In addition, the aerosol in all four air masses contains a significant fraction of organic material. This constantly high organics content in the measured aerosol, independent of the origin of the air masses could be the result of photochemically generated aerosol from vapors emitted from the forests on the Scandinavian peninsula.

This assumption is also supported by an observation during air mass #2. As shown in Figure 1, the lowest particle number concentrations were measured during the beginning of this time interval, down to a few hundred particles per cubic centimeter. Later during this time interval, in the afternoon of July 6, the particle number concentrations increased rapidly to approximately $3,500 \text{ cm}^{-3}$ while the aerosol mass concentrations increased only slightly. This behavior of the measured aerosol suggests that on this afternoon particle

Figure 3 Species-resolved mass distributions for the first half (a) and second half (b) of July 6. Before noon the size distributions barely exceed the noise level; after noon a distinct organics and sulfate size distribution appears as a result of new particle generation.



nucleation occurred upwind in the vicinity of the measurement site, generating a large amount of very small particles, similar to those events observed also with a Q-AMS by Allan et al. (2006) in a rural location in Southern Finland. In Figure 3 the species-resolved mass distributions for the species measured with the Q-AMS are shown, averaged for the first and second half of this day. While during the first half of the day the measured size distributions barely exceed the noise level of the Q-AMS, during the second half of the day a distinct size distribution is found for organics and sulfate with mode diameters at 180 and 230 nm, respectively. The peak in the organics size distribution in Figure 3a seems to be caused by a few randomly measured individual particles that accidentally had similar particle sizes. Especially total organics shows a prominent size distribution in the afternoon with very low mode diameter, compared to the remaining time of the measurements, suggesting that photooxidation of emitted organic vapors—very likely supported by condensation of sulfuric acid—is mainly involved in the generation and growth of the new particles. However, due to the fact that the Q-AMS does not measure particles in the lower nanometer range with sufficient sensitivity, one cannot conclude from these measurements whether the actual particle nucleation was caused by sulfuric acid or organic species or a combination of them.

The aerosol in the four time intervals was further characterized by analyzing the contributions of individual m/z to the total signal of some of the species. Pure ammonium nitrate particles generate a nitrate fragmentation pattern that consists mainly of signal at m/z 30 and 46 at a ratio of approximately 2:1 (Allan et al., 2003; Hogrefe et al., 2004). Laboratory experiments have shown a larger m/z 30:46 ratio for other inorganic nitrates, organic nitrates or organic nitrogen-containing species (Alfarra, 2004; Drewnick, 2002; Allan et al., 2006). For each averaging interval the ratio of the nitrate signal at m/z 30 to the nitrate signal at m/z 46 was calculated and the average ratio as well as the standard

Table III Parameters calculated for the aerosol of each of the four air masses for detailed characterization

Parameter	Air mass #1	Air mass #2	Air mass #4	Air mass #5
<i>m/z</i> 30/46 ratio (5%–95%)	4.9 ± 2.4	3.5 ± 5.5	4.4 ± 1.5	2.8 ± 3.1
<i>m/z</i> 44–organics ratio (5%–95%)	0.08 ± 0.01	0.11 ± 0.09	0.08 ± 0.01	0.09 ± 0.04
Nitrate – mode diameter/nm	270	295	320	305
Sulfate – mode diameter/nm	375	280	410	375
Ammonium – mode diameter/nm	340	280	370	350
Organics – mode diameter/nm	280	220	335	300

The *m/z* 30:46 ratio gives additional information on the nature of the measured nitrates; the *m/z* 44–organics ratio is a measure for the oxidation level of the aerosol; for calculation of both ratios only the 5%–95% data were used to avoid biases by ratios calculated from very low mass concentration data; mode diameters of the size distributions give information on the age of the particles. The uncertainties of the mode diameters are 5% in all cases, resulting in uncertainties ranging from 10 to 20 nm.

deviation of the ratios were calculated for every time interval individually (Table III). The ratios of the two nitrate fragments were in the range of 3.5 to 4.9 for air masses #1, 2, and 4 with a large uncertainty in air mass #2, where the absolute concentrations were very low. Air mass #5, where air influenced by the British Islands was measured had an average ratio of 2.8. A systematic bias of the nitrate fragmentation pattern due to fragments of the intensive organic contribution to the mass spectra can be ruled out. Therefore we assume that a fraction of the nitrate signal is generated by organic nitrates or other nitrogen-containing organic species (e.g., amines), similarly as observed by another group that used a Q-AMS to measure the ambient aerosol in Southern Finland a few months before these measurements (Allan et al., 2006) and similar to Q-AMS measurements in smog chamber experiments (Alfarra et al., 2006). The large amount of scatter in the ratios indicates that the fraction of ammonium nitrate and organic nitrates varies during the measurements. The low *m/z* 30:46 ratio for air mass #5 could be due to an increased ammonium nitrate content and less influence by Scandinavian forests in this air mass, such that a smaller fraction of the measured nitrate is organic nitrate that was generated by photochemical processes on the Scandinavian Peninsula.

Additional information on the aerosol composition was drawn from the analysis of the *m/z* 44 content of the organic aerosol fraction. The signal at *m/z* 44 is typically identified as CO₂⁺, which is a fragmentation product of oxidized organic species (Zhang et al., 2005). The larger the *m/z* 44 content of the organic aerosol, the larger the level of oxidation of the aerosol. The average *m/z* 44 to organics ratio for each of the air masses is also given in Table III. In air mass #1 and 4 approximately 8% of the organics signal is found at *m/z* 44; in air mass #2 the average fraction is 11% and in air mass #5 it is 9%. Thus the aerosol in the two air masses that contain the very large fraction of organics seems to be slightly less oxidized than the organic aerosol fraction in the other air masses. This could also be a consequence of relatively freshly generated organic aerosol, for example from organic vapors emitted by Scandinavian forests.

Generally the *m/z* 44 to organics ratio found for all four air masses is at a medium level, compared to other Q-AMS measurements. The lowest ratios are found in fresh diesel exhaust with about 5% *m/z* 44 of total organics (Schneider et al., 2006b). Ratios in the order of 8% to 10% were found in various studies at semi-urban and urban locations like Mainz, Germany or New York City. The most oxidized aerosol was found in the free troposphere and in remote areas in measurements on the Mt. Jungfrauoch in the Alps and on Crete (Schneider, 2005) with about 20% of the organics signal found at *m/z* 44.

Average species-resolved mass distributions were calculated for nitrate, sulfate, ammonium, and organics for each of the four time intervals individually and compared to each other. For direct comparison of distribution parameters monomodal log-normal distributions were fitted to each of the size distributions. The mode diameters, extracted from the fits to the distributions are also presented in Table III. For each of the air masses the mode diameter of the ammonium size distribution is found between those for nitrate and sulfate. This is a consequence of the fact that ammonium typically either appears as ammonium sulfate or ammonium nitrate and therefore its size distribution is related to the distributions of both species. The lowest mode diameter is found for the nitrate and organics size distributions for all air masses with the exception of air mass #2, where the nitrate distribution has the largest mode diameter of all species. This general trend indicates that nitrate and organic particles are typically the youngest particles of the sampled aerosol. Only in air mass #2, where most of the aerosol was very likely generated relatively freshly and therefore is found at small particle diameters, the nitrate mode is found above the mode diameters of the other species even though it is found at a similar diameter as in the other time intervals.

This general behavior of the size distribution of the individual species suggests that nitrate and organics are typically species from particles probably generated relatively shortly before being measured on Mt. Åreskutan. Very likely these species are the result of photooxidation processes of organic vapors, emitted from the forests in central Scandinavia or in Southern Finland. We assume that a significant fraction of the observed nitrate is either organic nitrates or other organic nitrogen-containing species. Sulfate on the other hand seems to be an older part of the ambient aerosol, which was not added in significant amounts to the aerosol in the region around the measurement site. Most of the sulfate is assumed to be introduced into the aerosol while the air masses passed over Eastern Europe or over the British Islands.

3.2 Cloud activation of aerosol particles

During several cloud events, i.e., times when the measurement station was within clouds, the composition of cloud droplet residuals was analyzed with the Q-AMS using the CVI to sample and evaporate only the cloud droplets. During parts of these cloud events the interstitial aerosol was also investigated by operating the CVI without the wind tunnel and the counterflow. During the whole campaign a total of 33.5 h of residual particle measurements were performed. This equals 5% of the total time of the campaign. Most of the cloud events occurred during the last week of measurements when air mass #5 was sampled. A minor fraction of the residual particle data was collected during air mass #2.

The average composition of the ambient, interstitial and residual aerosol during air mass #2 and 5 are shown in Table IV. Since in different air masses the aerosol was found to be significantly different from each other all measurements of residual particles, interstitial aerosol, and ambient aerosol were averaged for each air mass time interval separately. However, since ambient, interstitial, and residual aerosol were measured at different time intervals, the sum of interstitial and residual aerosol concentration does not have to be identical to the measured ambient concentration.

The mass concentrations of the residual aerosol, shown in Table IV, are calculated from the measured mass concentrations during CVI operation, divided by 11, the average enrichment factor of the CVI. During both time intervals the average residual particle mass concentration is about 3%–4% of the average total ambient aerosol mass concentration. Thus only a minor fraction of the total aerosol mass is activated to cloud droplets larger

Table IV Average mass concentrations of several non-refractory aerosol components for the ambient, interstitial and residual aerosol, measured with the Q-AMS during time interval #2 and 5

	Ambient		Interstitial		Residual	
Air Mass #2						
Nitrate	0.14 $\mu\text{g m}^{-3}$	3.6%	0.19 $\mu\text{g m}^{-3}$	4.1%	0.006 $\mu\text{g m}^{-3}$	4.5%
Sulfate	1.15 $\mu\text{g m}^{-3}$	30.3%	1.6 $\mu\text{g m}^{-3}$	34.0%	0.018 $\mu\text{g m}^{-3}$	13.6%
Ammonium	0.55 $\mu\text{g m}^{-3}$	14.0%	0.75 $\mu\text{g m}^{-3}$	15.9%	0.012 $\mu\text{g m}^{-3}$	9.1%
Organics	2.0 $\mu\text{g m}^{-3}$	52.1%	2.1 $\mu\text{g m}^{-3}$	46.0%	0.10 $\mu\text{g m}^{-3}$	72.8%
Total	3.8 $\mu\text{g m}^{-3}$	100%	4.7 $\mu\text{g m}^{-3}$	100%	0.13 $\mu\text{g m}^{-3}$	100%
Number Conc.	900 cm^{-3}	–	290 cm^{-3}	–	1.2 cm^{-3}	–
Air Mass #5						
Nitrate	0.39 $\mu\text{g m}^{-3}$	2.6%	0.33 $\mu\text{g m}^{-3}$	2.9%	0.05 $\mu\text{g m}^{-3}$	10.5%
Sulfate	5.4 $\mu\text{g m}^{-3}$	35.7%	4.7 $\mu\text{g m}^{-3}$	41.0%	0.12 $\mu\text{g m}^{-3}$	23.8%
Ammonium	1.9 $\mu\text{g m}^{-3}$	12.8%	1.55 $\mu\text{g m}^{-3}$	13.6%	0.06 $\mu\text{g m}^{-3}$	12.3%
Organics	7.3 $\mu\text{g m}^{-3}$	48.9%	4.8 $\mu\text{g m}^{-3}$	42.5%	0.27 $\mu\text{g m}^{-3}$	53.4%
Total	15.0 $\mu\text{g m}^{-3}$	100%	11.4 $\mu\text{g m}^{-3}$	100%	0.5 $\mu\text{g m}^{-3}$	100%
Number Conc.	920 cm^{-3}	–	830 cm^{-3}	–	10 cm^{-3}	–

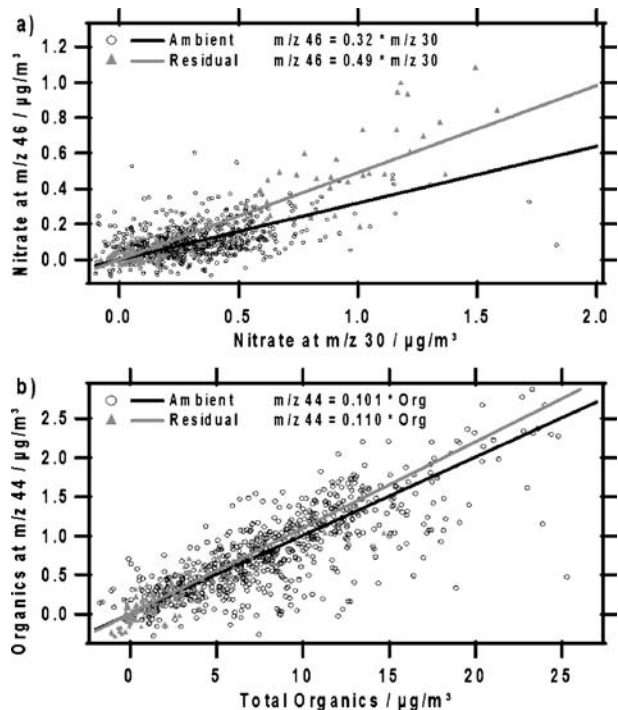
Average particle number concentrations for each aerosol type and time interval, measured with the CPC. The residual concentrations were calculated from the measured concentrations by dividing with 11, the average CVI enrichment factor. The absolute mass concentration data have an uncertainty of $\sim 25\%$, the relative concentrations have an uncertainty of $\sim 5\%$.

than approximately 5 μm diameter. In terms of particle number concentration the situation is slightly different: During air mass #2 only about 0.13% of the particles are activated (by number) while during air mass #5 about 1.1% of the particles are found to be activated, indicating that during this time interval a smaller fraction of very small aerosol particles existed, that contained only a very small mass fraction while making up a significant fraction of the number concentration.

During both time intervals only very minor differences are found between the absolute and relative composition of the particles of the ambient and interstitial aerosol. However, in addition to the fact that the total mass concentrations of the residual particles are much lower than those of the ambient aerosol, also the average relative composition of the residual particles is significantly different from those of the ambient particles, indicating that some of the species end up in cloud droplets with higher probability than others. For both air masses the nitrate fraction found in the residual particles is larger than that found in the ambient aerosol. While in air mass #2 only a slight enhancement of the nitrate content is found, in air mass #5 the residual nitrate fraction is more than four times larger than the ambient nitrate fraction. Also for organics, which was typically the most prominent ambient aerosol component an increase in the relative content was found in the residual particles, compared to the ambient composition. As a consequence of the increase in relative nitrate and organics fraction the sulfate fraction was lower in the residual particles compared to the ambient aerosol for both time intervals.

These results suggest that nitrate as well as organic aerosol particles are more efficiently activated to form cloud droplets than sulfate particles. If we assume (partial) internal mixture of these species we have to express this more carefully: particles that contain a large amount of nitrate or organic species are more efficiently activated into cloud droplets than particles that contain a large amount of sulfate. An alternative process that would result in enhanced nitrate and organics fraction in the residual particles would be enrichment of these species in the cloud droplets by scavenging of their vapors. However, as we will see in the aerosol cloud processing section, this process can be ruled out as cause of this enhancement.

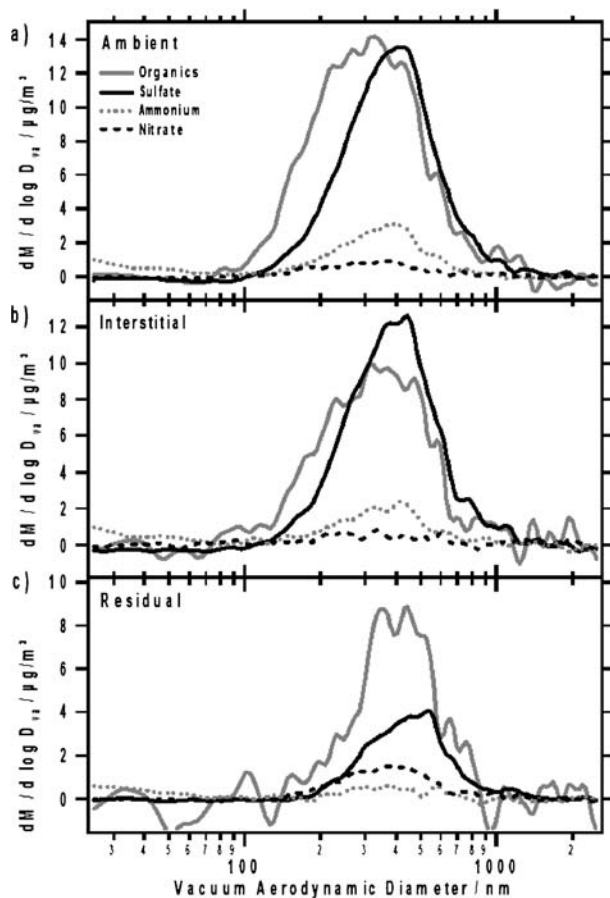
Figure 4 Correlations of the nitrate fragments at m/z 30 and m/z 46 for the ambient and residual particle measurements (a), and for the organics fragment at m/z 44 versus total organics for both aerosol types (b). Both correlations were calculated for the time interval of air mass #5.



More information about the composition of the residual particles was again drawn from the relative contribution of individual m/z to certain species mass concentrations. In Figure 4 correlation plots of the nitrate fragments m/z 30 and 46 and of the organics component m/z 44 versus total organics are shown for the ambient aerosol measurements and the residual particle measurements during air mass #5. As shown in Figure 4a we find a significant difference in the correlations of the nitrate fragments for the ambient and residual particles. As discussed before the average ratio of m/z 30 to m/z 46 signal is about 3:1 for the ambient particles during this time interval, indicating that a significant fraction of the nitrate signal is generated by organic nitrates or other organic nitrogen-containing components. However, for the residual particles the m/z 30 to m/z 46 signal ratio is about 2:1, the ratio that is expected for ammonium nitrate. This finding that ammonium nitrate is found with higher efficiency in the cloud droplet residuals than in the ambient particles suggests that ammonium nitrate particles or particles that contain a large fraction of ammonium nitrate are activated with significantly higher efficiency than particles that contain organic nitrates or other organic nitrogen-containing components. This is in good agreement with solubility data of ammonium nitrate and various organic components (Lide, 1999). Also in this case the possibility exists that ammonium nitrate is generated inside the cloud droplets from organic nitrates by scavenging of ammonia vapor. However, as we will see in the discussion of aerosol cloud processing below, this process can be ruled out.

A slightly different situation is found for the correlations between the organics signal at m/z 44 and the total organics signal as shown in Figure 4b. Here only a small and insignificant difference is found between the correlations for the ambient and the residual particles. For both aerosol types about 10%–11% of the organics is found at m/z 44, indicating that no part of the organic aerosol is incorporated into the cloud droplets with higher efficiency. However, this does not allow us to conclude that all organic aerosol

Figure 5 Averaged species-resolved mass distributions for the ambient, interstitial, and residual aerosol during air mass #5. Due to short averaging times the data were slightly smoothed to reduce noise.



components are activated into cloud droplets with the same efficiency since differences in the activation efficiency for different organic aerosol components could be covered by internal mixing of the components in the aerosol particles or by differences in the size distributions for the different components.

Some information about the size-dependency of aerosol cloud activation for the individual species can be extracted from the species-resolved aerosol mass distributions. Since only during time interval #5 sufficient measurements of residual particles were obtained to allow calculation of average size distributions, only these data were used for further analysis. In Figure 5 the average species-resolved mass distributions for ambient, interstitial, and residual particles are shown. Monomodal log-normal distributions were fitted to the size distribution of each species for each aerosol type. The mode diameters and geometric standard deviations (GSDs) of the distributions calculated from these fits are presented in Table V.

According to Table V no clear trend is found for the width of the mass distributions: while for the ammonium distribution the GSD for the residual particles does not differ from those of the interstitial or ambient aerosol, for the other species a slightly smaller distribution width is found for the residual particles. This could be due to the activation of only the larger particles within the initial (ambient) size distribution. A more consistent

Table V Mode diameters and geometric standard deviations for each species and each aerosol type, calculated from monomodal log-normal distributions fitted to the average measured mass distributions for time interval #5

	Ambient		Interstitial		Residual	
	Mode (nm)	GSD	Mode (nm)	GSD	Mode (nm)	GSD
Ammonium	350	1.64	355	1.63	365	1.64
Nitrate	305	1.88	320	2.00	360	1.79
Sulfate	375	1.73	380	1.70	440	1.65
Organics	300	2.00	330	1.91	400	1.60

The uncertainties of the mode diameters are in the order of 5% (15–20 nm); the uncertainties of the GSDs are ± 0.05 .

behavior is found for the mode diameters. For all species a slight increase of the mode diameter is found from the ambient to the interstitial mass distributions, ranging from 5 nm for ammonium and sulfate to 30 nm for organics. This increase in mode diameter could be caused by limited water uptake by the non-activated aerosol particles during cloud events or by collision scavenging of the smallest unactivated particles by the cloud droplets (Noone et al., 1992). Another larger difference in mode diameter is found between the interstitial particles and the residual particles. This difference is at average 45 nm, ranging from 10 nm for ammonium up to 70 nm for organics.

We assume that these differences in mode diameter between the interstitial aerosol and the residual aerosol are caused by preferential activation of larger aerosol particles into cloud droplets. We are not able to extract exact activation cut-off diameters from the data, however, from the mass distributions presented in Figure 5c we can estimate lower cut-off diameters above which a significant amount of aerosol mass is activated into cloud droplets. From these distributions we estimate this mass-based cut-off diameter to be approximately $d_{va} \approx 150$ nm (vacuum aerodynamic diameter) for organics and nitrate and $d_{va} \approx 200$ nm for sulfate. Since ammonium is associated with both nitrate and sulfate we do not provide an extra activation diameter for this species. Again these findings suggest that particles that contain large amounts of nitrate or organics are activated into cloud droplets with higher efficiency than particles that contain large amounts of sulfate.

3.3 Cloud processing of the ambient aerosol

For investigation of aerosol cloud processing the ambient aerosol was compared for time intervals just before and just after cloud events. During the campaign, two cloud events were observed where the ambient aerosol was measured before as well as after the cloud surrounded the measurement station. Cloud event #1 was observed on July 23 between 10:00 and 12:00 local time. The second cloud (cloud event #2) was observed on July 26 between 22:00 and July 27 10:30 local time (Figure 1). While we do not have any information about the nature of the first cloud, the second cloud had its base only slightly below the measurement site and some drizzle was observed during this cloud event. For determination of the ambient aerosol compositions always the 5 h of ambient measurement before and after the cloud event were used.

The absolute mass concentrations of the non-refractory species, measured with the Q-AMS and the relative composition of the aerosol before and after the two cloud events are shown in Figure 6. The uncertainty of the absolute mass concentration measurement with

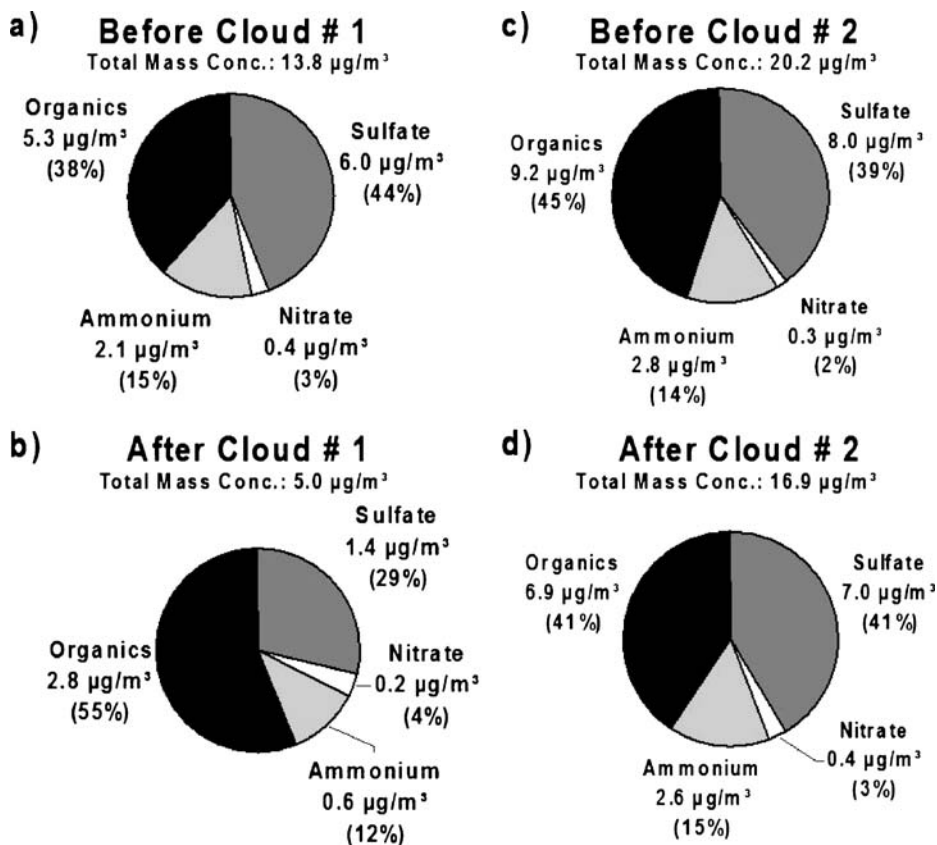


Figure 6 Mass concentrations and relative composition of sulfate, nitrate, ammonium and total organics for the ambient aerosol before and after two cloud events (see text).

the Q-AMS is in the order of 25%, the uncertainty of the relative mass concentration data is approximately 5% of the measured value for nitrate, sulfate, and organics, and slightly more for ammonium. While after cloud event #1 (Figure 6a, b) the total aerosol mass concentration dropped to almost a third of its pre-cloud value, it decreased only by 16% during the second cloud event (Figure 6c, d). This could be due to intensive rain during cloud #1 or due to a change in air mass between the pre- and post-cloud aerosol for this event.

A similar situation is found for the changes in relative composition of the ambient aerosol from before to after the cloud event: while for cloud #1 the relative composition changes significantly, no considerable change of the composition of the ambient aerosol is found for cloud event #2. After cloud #1 the organics content has increased from 38% to 55% while the sulfate fraction decreased from 44% to 29%. Ammonium followed the sulfate trend and the nitrate fraction has remained almost constant. These numbers suggest that ammonium sulfate was ‘consumed’ by the cloud with higher efficiency than organic species. However, these results have to be taken with care since an air mass change cannot be excluded for this cloud event and no such change was apparent for cloud #2. We therefore conclude that we cannot find proof for any change in the relative composition of the ambient aerosol as a consequence of a cloud passing through the measurement site. However, using these findings we can exclude that the enhancement of nitrate or organics

Table VI Parameters of the species-resolved size distributions of the ambient aerosol before and after cloud event #1 and 2

	Cloud event #1				Cloud event #2			
	Before cloud		After cloud		Before cloud		After cloud	
	Mode (nm)	GSD	Mode (nm)	GSD	Mode (nm)	GSD	Mode (nm)	GSD
SO ₄	395	1.73	305	(1.23)	375	1.73	360	1.65
NO ₃	(280)	(1.36)	–	–	335	1.86	310	1.69
HN ₄	335	1.98	–	–	345	1.66	335	1.54
Org	(390)	(1.20)	(245)	(6.03)	325	1.93	335	1.78

During cloud event #1 the particle mass concentrations were so low that only uncertain (values in parenthesis) or no log-normal distributions could be fitted to the size distributions.

found in the residual particles is caused by scavenging of vapors by cloud droplets as hypothesized above.

Comparison of the nitrate fragmentation pattern before and after the cloud events did not show a significant increase of the signal ratio at m/z 46 to m/z 30 of about 1:3 before and after the cloud events. Thus the hypothesis that ammonium nitrate is enriched in the cloud droplets compared to the ambient aerosol as a consequence of scavenging of ammonia can also be excluded.

Average size distributions were calculated for the same time intervals before and after the two cloud events for each of the species individually. In order to compare the size distributions before and after the cloud monomodal log-normal distributions were fitted to each of the distributions. The mode diameter and the width (GSD) of the distributions are given in Table VI. The uncertainties of the mode diameters are in the order of 5% (15–20 nm); the uncertainties of the GSDs are ± 0.05 . For some of the size distributions of cloud #1 the aerosol mass concentrations were so low that the calculated parameters of the distributions are either uncertain (parameter given in parenthesis) or that it was even not possible to generate a meaningful fit to the data (no parameter given).

The parameters presented in Table VI show that the mode diameters of the individual size distributions tend to be smaller after the cloud event, compared to before the event. Parallel to this development the widths of the size distributions decreases over the cloud event for all species. These results indicate that preferentially large particles are activated into cloud droplets and disappear from the aerosol as a consequence of precipitation. With increasing particle size the activation efficiency increases such that very large particles are removed by the cloud with high probability and as a consequence the width of the size distribution is reduced.

4 Summary

The combination of the Aerodyne aerosol mass spectrometer (Q-AMS) with the CVI inlet deployed during the study on Mt. Åreskutan has proven to be a valuable tool for measuring the ambient aerosol and cloud droplet residuals. The ambient aerosol at the measurement site showed to be mainly influenced by the origin of the air masses advected to the area. During the measurement campaign four air masses were distinguished and further analyzed. The aerosol measured during two time intervals where the air masses originated in northeastern Europe and approached the measurement site via Finland were similar in

composition while the aerosol of the two other air masses was significantly different. In all air masses the organic aerosol fraction dominated the total mass, while nitrate comprises only a minor fraction. The analysis of the nitrate fragmentation pattern revealed that a significant but varying fraction of the measured nitrate is not ammonium nitrate but organic nitrates or other nitrogen-containing organic species. The mass concentration measurements as well as the measurements of species-resolved mass distributions indicate that a significant fraction of the ambient nitrate and organics is relatively freshly generated, possibly as secondary aerosol from emissions from Scandinavian forests, while the sulfate component seems to be a more aged component of the aerosol that was mainly found when the air masses passed continental Europe or Great Britain. Generally the organic aerosol component shows, compared to other Q-AMS measurements, a medium level of oxidation with approximately 10% to 11% of the organics signal found at m/z 44, which is comparable with measurements made in semi-urban or urban locations.

Measurements of residual particles showed that about 3.5% of the ambient aerosol mass was incorporated into cloud droplets larger than 5 μm diameter during the two cloud events that were analyzed in more detail. Comparison of Q-AMS mass concentration measurements with particle number concentration measurements as well as species-resolved mass concentrations revealed that mainly the larger aerosol particles are activated into cloud droplets. Activation diameters were estimated on a mass basis to be $d_{va} = 150$ nm for nitrate and organic dominated particles; for sulfate-dominated particles an activation diameter of $d_{va} = 200$ nm was estimated. Also the composition of the residual particles indicated that nitrate and organics were more efficiently incorporated into cloud droplets than sulfate. The analysis of the nitrate fragmentation pattern showed that the nitrate found in the cloud droplets is mainly ammonium nitrate, different than the nitrate found in the ambient aerosol.

Cloud processing of the aerosol was investigated by comparison of the ambient aerosol composition and size distributions just before and after cloud events. This analysis did not show any clear changes of the ambient aerosol composition as a consequence of cloud passage. However, the size distributions showed a significant reduction in mode diameter and distribution width as a consequence of preferential activation and removal of larger aerosol particles by precipitation.

Acknowledgments We like to thank the Institute of Applied Environmental Research at Stockholm University for providing access to the Åreskutan sampling facility. We also thank the Swedish Weather Service for providing meteorological data for the Åreskutan area. We want to acknowledge the European Center of Medium-range Weather Forecasts (ECMWF) for providing the 2001 version of the McGrath air trajectory model, which was used to calculate the back-trajectories for this study. Funding for the measurement campaign is acknowledged from internal grants of Max-Planck Institute for Chemistry and University of Mainz.

References

- Albrecht, B.A.: Aerosols, cloud microphysics, and fractional cloudiness. *Science* **245**, 1227–1230 (1989)
- Alfarra, M.R.: Insights into atmospheric organic aerosols using an aerosol mass spectrometer, PhD thesis, University of Manchester, Institute of Science and Technology (UMIST), UK (2004)
- Alfarra, M.R., Paulsen, D., Gysel, M., Garforth, A.A., Dommen, J., Prevot, A.S.H., Worsnop, D.R., Baltensperger, U., Coe, H.: A mass spectrometric study of secondary organic aerosols formed from the photooxidation of anthropogenic and biogenic precursors in a reaction chamber. *Atmos. Chem. Phys.* **6**, 7747–7789 (2006)

- Allan, J.D., Jimenez, J.L., Williams, P.I., Alfarra, M.R., Bower, K.N., Jayne, J.T., Coe, H., Worsnop, D.R.: Quantitative sampling using an Aerodyne aerosol mass spectrometer – 1. Techniques of data interpretation and error analysis. *J. Geophys. Res. – Atmospheres* **108**, 4090, <http://dx.doi.org/10.1029/2002JD002358> (2003)
- Allan, J.D., Delia, A.E., Coe, H., Bower, K.N., Alfarra, M.R., Jimenez, J.L., Middlebrook, A.M., Drewnick, F., Onasch, T.B., Canagaratna, M.R., Jayne, J.T., Worsnop, D.R.: A generalised method for the extraction of chemically resolved mass spectra from Aerodyne aerosol mass spectrometer data. *J. Aerosol Sci.* **35**, 909–922 (2004)
- Allan, J.D., Alfarra, M.R., Bower, K.N., Coe, H., Jayne, J.T., Worsnop, D.R., Aalto, P.P., Kulmala, M., Hyötyläinen, T., Cavalli, F., Laaksonen, A.: Size and composition measurements of background aerosol and new particle growth in a Finnish forest during QUEST 2 using an aerdyne aerosol mass spectrometer. *Atmos. Chem. Phys.* **6**, 315–327 (2006)
- DeCarlo, P., Slowik, J.G., Worsnop, D.R., Davidovits, P., and Jimenez, J.L.: Particle morphology and density characterization by combined mobility and aerodynamic diameter measurements. Part 1: theory. *Aerosol Sci. Tech.* **38**, 1185–1205 (2004)
- Drewnick, F.: Results presented on the 2. AMS Users Meeting, October 2002. Billerica, Massachusetts, USA (2002)
- Drewnick, F., Schwab J.J., Jayne, J.T., Canagaratna, M., Worsnop, D.R., Demerjian, K.L.: Measurement of ambient aerosol composition during the PMTACS-NY 2001 using an aerosol mass spectrometer. Part I: mass concentrations. *Aerosol Sci. Tech.* **38**, 92–103 (2004)
- Drewnick, F., Hings S.S., DeCarlo, P., Jayne, J.T., Gonin, M., Fuhrer, K., Weimer, S., Jimenez, J.L., Demerjian, K.L., Borrmann, S., Worsnop, D.R.: A new Time-of-Flight Aerosol Mass Spectrometer (TOF-AMS)-Instrument description and first field deployment. *Aerosol Sci. Tech.* **39**, 637–658 (2005)
- Gieray, R., Greiner, W., Wieser, P.H.: Laser microprobe mass analysis of fog droplet residues. *J. Aerosol Sci.* **20**, 1209–1212 (1989)
- Hallberg, A., Noone, K.J., Ogren, J.A., Svenningsson, I.B., Flossmann, A., Wiedensohler, A., Hansson, H.-C., Heintzenberg, J., Anderson, T., Arends, B., Maser, R.: Phase partitioning of aerosol particles in clouds at Kleiner Feldberg. *J. Atmos. Chem.* **19**, 107–127 (1994)
- Hogrefe, O., Drewnick, F., Lala, G.G., Schwab, J.J., Demerjian, K.L.: Development, operation and applications of an aerosol generation, calibration and research facility. *Aerosol Sci. Tech.* **38**(S1), 196–214 (2004)
- Houghton, J.T., Ding, Y., Griggs, D.J., Noguier, M., van der Linden, P.J., Dai, X., Maskell, K., Johnson, C.A. (eds.): *Climate Change 2001: The Scientific Basis-Contribution of Working Group I to the Third Assessment Report of the Intergovernmental Panel on Climate Change*. Cambridge University Press, New York (2001)
- Jayne, J.T., Leard, D.C., Zhang, X., Davidovits, P., Smith, K.A., Kolb, C.E., Worsnop, D.R.: Development of an aerosol mass spectrometer for size and composition, analysis of submicron particles. *Aerosol Sci. Tech.* **33**, 49–70 (2000)
- Jimenez, J.L., Jayne, J.T., Shi, Q., Kolb, C.E., Worsnop, D.R., Yourshaw, I., Seinfeld, J.H., Flagan, R.C., Zhang, X., Smith, K.A., Morris, J., Davidovits, P.: Ambient aerosol sampling with an aerosol mass spectrometer. *J. Geophys. Res. – Atmospheres* **108** (D7), 8425, <http://dx.doi.org/10.029/2001JD001213> (2003a)
- Jimenez, J.L., Bahreini, R., Cocker, D.R., Zhuang, H., Varutbangkul, V., Flagan, R.C., Seinfeld, J.H., O'Dowd, C., Hoffmann, T.: New particle formation from photooxidation of diiodomethane (CH₂I₂). *J. Geophys. Res. – Atmospheres* **108**(D10), 4090 (2003b)
- Kulmala, M., Vehkamäki, H., Petäjä, T., Dal Maso, M., Lauri, A., Kerminen, V.-M., Birmili, W., McMurry, P. H.: Formation and growth rates of ultrafine atmospheric particles: a review of observations. *J. Aerosol Sci.* **35**, 143–176 (2004)
- Lide, D.R. (ed.): *Handbook of Chemistry and Physics* (80th Edition). CRC Press, Boca Raton, Florida (1999)
- Noone, K.J., Ogren, J.A., Heintzenberg, J., Charlson, R.J., Covert, D.S.: Design and calibration of a counterflow virtual impactor for sampling of atmospheric fog and cloud droplets. *Aerosol Sci. Tech.* **8**, 235–244 (1988)
- Noone, K.J., Ogren, J.A., Noone, K.B., Hallberg, A., Fuzzi, S., Lind, J.A.: Measurements of the partitioning of hydrogen-peroxide in a stratiform cloud. *Tellus* **43B**, 280–290 (1991)
- Noone, K.J., Ogren, J.A., Hallberg, G.A., Heintzenberg, J., Ström, J., Hansson, H.C., Svenningsson, B., Wiedensohler, A., Fuzzi, S., Facchini, M.C., Arends, B.G., Berner, A.: Changes in aerosol size and phase distributions due to chemical and physical processes in fog. *Tellus* **44B**, 489–504 (1992)
- Noone, K.J., Ostrom, E., Ferek, R.J., Garrett, T., Hobbs, P.V., Johnson, D.W., Taylor, J.P., Russell, L.M., Flagan, R.C., Seinfeld, J.H., O'Dowd, C.D., Smith, M.H., Durkee, P.A., Nielsen, K., Hudson, J.G.,

- Pockalny, R.A., De Bock, L., Van Grieken, R.E., Gasparovic, R.F., Brooks, I.: A case study of ships forming and not forming tracks in moderately polluted clouds. *J. Atmos. Sci.* **57**, 2729–2747 (2000)
- Ogren, J.A., Heintzenberg, J., Charlson, R.J.: In situ sampling of clouds with a droplet to aerosol converter. *Geophys. Res. Lett.* **12**, 121–124 (1985)
- Ogren, J.A., Heintzenberg, J., Zuber, A., Noone, K.J., Charlson, R.J.: Measurements of the size-dependence of solute concentrations in cloud droplets. *Tellus* **41B**, 24–31 (1989)
- Schneider, J.: Unpublished Results (2005)
- Schneider, J., Hings, S.S., Hock, B.N., Weimer, S., Borrmann, S., Fiebig, M., Petzold, A., Busen, R., Kärcher, B.: Aircraft-based operation of an aerosol mass spectrometer: Measurements of tropospheric aerosol composition. *J. Aerosol Sci.* **37**, 839–857, 2006a, doi:[10.1016/j.jaerosci.2005.07.002](https://doi.org/10.1016/j.jaerosci.2005.07.002)
- Schneider, J., Weimer S., Drewnick, F., Borrmann, S., Helas, G., Gwaze, P., Schmid, O., Andreae, M.O., Kirchner U.: Mass spectrometric analysis and aerodynamic properties of various types of combustion-related aerosol particles. *Int. J. Mass. Spec.* in press, 2006b, doi:[10.1016/j.ijms.2006.07.008](https://doi.org/10.1016/j.ijms.2006.07.008)
- Twomey, S.: Minimum size of particle for nucleation in clouds. *J. Atmos. Sci.* **34**, 1832–1835 (1977)
- Zhang, Q., Alfara, M.R., Worsnop, D.R., Allan, J.D., Coe, H., Canagaratna, M.R., Jimenez, J.L.: Deconvolution and quantification of hydrocarbon-like and oxygenated organic aerosols based on aerosol mass spectrometry. *Eviron. Sci. Technol.* **39**, 4938–4952 (2005)